doi:10.2533/chimia.2011.691 Chimia 65 (2011) 691–695

Study of the pO_2-Sensitivity of the Dendrimeric and Free Forms of Pd-meso-tetra(4-carboxyphenyl)porphyrin, Incorporated or not in Chitosan-Based Nanoparticles

Patrycja Nowak-Sliwinska*[a], Peter Käuper[b], Hubert van den Bergh[ac], and Georges Wagnières*[c]

Abstract: The concentration of oxygen and its rate of consumption are important factors in certain medical treatments, such as radiotherapy and photodynamic therapy (PDT). Measuring the tissue concentration of oxygen or its partial pressure (pO_2) can be achieved by taking advantage of the oxygen-dependent luminescence lifetime of certain molecules, including metallo-porphyrin derivatives, due to the oxygen-dependent quenching of their triplet state. Unfortunately, most of these porphyrin derivatives are phototoxic due to the $O_2{}^1\Delta$ produced in the pO_2 measurement procedure. The aim of this work was to characterize new nanoparticle oxygen sensors, where the palladium-porhyrin molecule (Pd-meso-tetra(4-carboxyphenyl)porphyrin) or its dendrimer form, is incorporated into an oxygen permeable matrix of chitosan-based colloidal particles. It was hypothesized that the reactive $O_2{}^1\Delta$ produced during the pO_2 measurement would react inside the particle thus reducing its toxicity for the surrounding tissue, whereas the $^3\sum$ ground state of O_2, that is to be measured, would diffuse freely in the peptide. We observed that the incorporation of the porphyrin in the nanoparticles resulted in a reduction of the phosphorescence lifetime sensitivity to pO_2 by about one order of magnitude. Our studies of these new sensors indicate that the oxygen concentration can be measured in aqueous solutions with a precision of ±20% for oxygen concentrations ranging between 0% and 25%.

Keywords: Chitosan · Nanoparticle · Oxygen partial pressure · Oxyphor · Phosphorescence quenching

Introduction

Monitoring the tissue oxygenation before, during and after treatment is important to better understand the mechanisms and outcome of radiotherapy[1,2] and photodynamic therapy (PDT),[3–6] since pO_2 is involved in the processes leading to tissue destruction. Therefore, the ability to quantitatively and reliably measure the tissue oxygen concentration may help to optimize these therapeutic methods.[7–10] Measuring the oxygen partial pressure (pO_2) also provides valuable information regarding the tissue metabolism. This is of importance to understand the basic mechanisms involved in hypoxia-induced neovascular diseases, including age-related macular degeneration (AMD),[11,12] diabetic retinopathy,[13] as well as cancer.[1,14,15] Measuring pO_2 might even be used in the early detection of these conditions.

Time-resolved luminescence detection techniques for measuring pO_2 are in general more reliable than luminescence intensity-based methods.[16,17] For the type of O_2-sensing molecules we are concerned with here, the phosphorescence lifetime depends on the concentration of quenching molecules, including especially the molecular oxygen present in the solution.

Following the development of sensitive and non-invasive time-dependent optical spectroscopic techniques based on the *oxygen*-dependent luminescence quenching of selected molecular probes, the level of oxygenation can thus be measured quantitatively at selected sites.[18–20] Palladium-meso-tetra(4-carboxyphenyl) porphyrin (Oxyphor **R0**; see Fig. 1A) and its multimeric form, Pd-meso-tetra(4-carboxyphenyl) porphyrin dendrimer (Oxyphor **R2**; see Fig. 1B), are two of the molecules frequently used in this context.[20,21] Many of the known porphyrins are characterized by limited solubility in water. This drawback can be avoided by synthesizing porphyrin derivatives with multiple polar or charged groups.[22]

These oxygen probes generally present a relatively high phosphorescence quantum yield (Φ_{phos} = 6% for Oxyphor **R0** and Φ_{phos} = 12% for Oxyphor **R2**), long triplet state lifetimes (about 0.7 ms under anoxic conditions) in an aqueous environment, and a high absorption coefficient in the visible part of the spectrum (for Oxyphor **R0**, $\varepsilon_{410} = 2.5\times10^5$ [$M^{-1}cm^{-1}$]; and $\varepsilon_{524} = 1.9\times10^5$ [$M^{-1}cm^{-1}$] for Oxyphor **R2**).[23,24] Unfortunately, these oxygen probes are phototoxic, due to the production of $O_2{}^1\Delta$ in the triplet quenching process. This is the case for virtually all molecules based on the same pO_2-sensing mechanism, thus leading to tissue damages, including vascular damages, during the pO_2 measurements.[20] Thus, the measurement may strongly perturb the tissue in which one wants to measure the pO_2. Here we are trying to develop a strategy to incorporate these sensors in nanoparticle-based formulations, which should eventually enable pO_2 measurement *in vivo*. In this approach, to overcome phototoxicity, the molecular oxygen sen-

*Correspondence: Dr. P. Nowak-Sliwinska[a], Dr. G. Wagnières[c]
Tel.: +41 21 693 5169
Fax: +41 61 693 5110
E-mail: Patrycja.Nowak-Sliwinska@epfl.ch
[a]Institute of Bioengineering
Swiss Federal Institute of Technology (EPFL)
Station 6, CH-1015, Lausanne
[b]Medipol Ltd, PSE-B, CH-1015 Lausanne
[c]Institute of Chemical Sciences and Engineering,
Swiss Federal Institute of Technology (EPFL),
Station 6, CH-1015, Lausanne

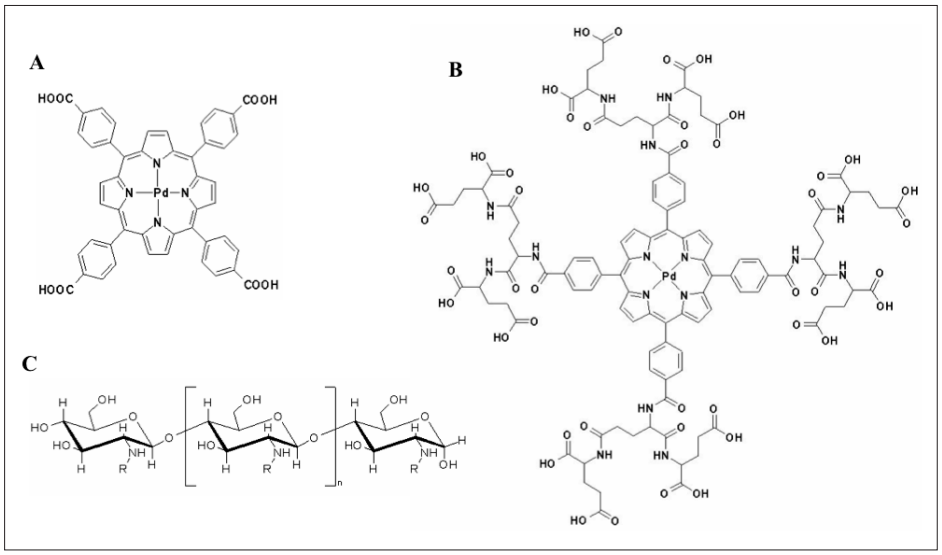

Fig. 1. Chemical structures of the Oxyphors **R0** (A) and **R2** (B), repeating units of chitin and chitosan: R = CH_3CO for chitin; R = H for chitosan (C).

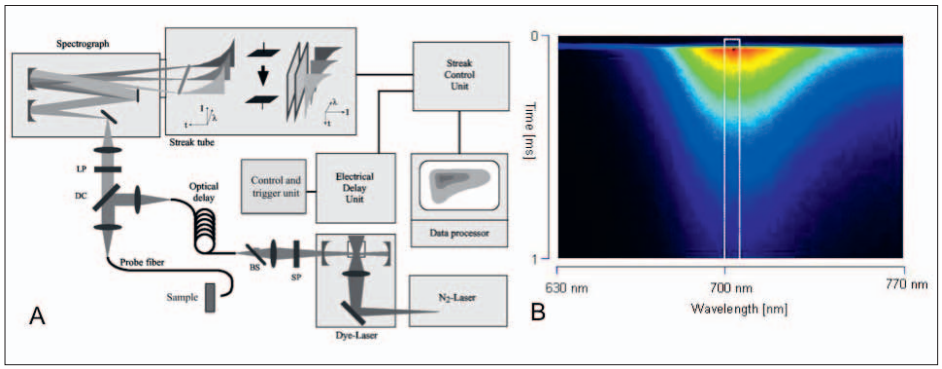

Fig. 2. Optical fiber-based time-resolved spectrophotometer. A) Block diagram of the experimental setup adapted from ref. [27]. BS: beam-splitter, DC: dichroic filter, LP: long pass filter, SP: short pass filter; B) Example of spectro-temporal recording from the streak camera. White-marked area in the spectrum is an example of the chosen spectral domain providing the highest intensity, from which the phosphorescence lifetime is extracted.

sors are incorporated in oxygen-permeable nanoparticles (NPs), in which the O_2 can diffuse easily. However, the tissue should be shielded from the toxic photoproducts, including singlet oxygen and/or radicals[25] produced by the oxygen sensor porphyrin complex in the measurement, by rapid reaction of the $O_2{}^1\Delta$ with the material of the NP. Consequently, there is a need, for oxygen permeable NPs that essentially do not affect the physico-chemical properties of the molecular oxygen probe. Among the ideal properties of such particles for the application considered here, is that they should be (i) non-toxic and well tolerated *in vivo*, (ii) mono-disperse enabling its homogenous distribution in blood, and (iii) stable, from a photochemical, and immunological point of view and have an optimal circulation time in the body. Biodegradable matrixes composed of polyesters or polysaccharides are interesting candidates for this purpose. NPs composed of the polysaccharide chitosan as main component are interesting candidates.[26]

Therefore, the main goal of the present work was to develop and study new nanosensors for pO_2 measurement encapsulated in such particles. More precisely, we report on the phosphorescence lifetime measurement (Fig. 2) of Oxyphor **R0** and Oxyphor **R2**, incorporated or not in chitosan-based NPs with different O_2 permeability, polyanion carrier, and zeta potential.

Results and Discussion

Optical Spectroscopy

As stated above, the purpose of the incorporation of Oxyphor **R0** or **R2** into chitosan-based nanoparticles was to shield the tissue in which the sensor is measuring pO_2 from the toxic $O_2{}^1\Delta$. For these Oxyphor-based sensors the spectral regions 380–420 nm (Soret band) and 515–535 nm (Q-band) can be used for excitation. The Soret band of the absorption spectrum of NP2 (room temperature, 21% of oxygen) in aqueous solutions appeared to be shifted hypsochromically as compared to the Soret band of Oxyphor **R0**, whereas the Q-band showed a very small bathochromic shift (see Fig. 3A). In the case of NP4, a bathochromic shift for both the Soret and the Q-bands was observed, as compared to those of Oxyphor **R2** (Fig. 3B). These two figures are presented to illustrate the spectral changes we observed typically after the incorporation of the Oxyphors in the chitosan NPs. The spectral data are given for all compounds in Table 1. Similarly, the emission bands of both Oxyphors and NP in PBS (pH 7.3, room temperature, 21% of oxygen) are given in Table 1. The spectra given in the Fig. 3C were obtained with **R0** and NP2, and they illustrate the typical spectral modification observed in two oxygenation conditions. The incorporation of Oxyphors **R0** or **R2** in NPs induced a small bathochromic shift of the fluorescence bands as compared to their free forms (Fig. 3 and Table 1). The ratio of the value of fluorescence over phosphorescence intensity of these peaks differed for each nanoparticle formulation (Table 1). The emission spectra of free Oxyphor **R0** exhibited a highly oxygen-dependent phosphorescence intensity (700–715 nm). At room conditions (21% of oxygen), the fluorescence over phosphorescence ratio is 2:1 (see curve 4, Fig. 3C), whereas in deoxygenated environment (0% of oxygen) this ratio was much more smaller (about 1:8) due to the reduced quenching of the triple state (see curve 1, Fig. 3C). For NP formulations of Oxyphor **R0** (see, as illustration, the case of NP2 in Fig. 3C) at 21% of oxygen, the phosphorescence was less quenched, as compared to the free forms of the Oxyphors. This could be due to the fact that, inside the nanoparticles, the oxygen diffusion is not as efficient as for the solution in which are dissolved the free forms of the Oxyphors. This limited diffusion of oxygen in the NPs material possibly also explains the difference of phosphorescence intensity with 0% of oxygen. For free Oxyphor **R2**, the fluorescence over phosphorescence ratio was 2:1 (Table 1), and was reduced by a factor 3 under nitrogen-saturated conditions (data not shown).

Time-resolved Measurements

Subsequently, Oxyphors phosphorescence lifetime measurements were measured in solutions at known oxygen concentrations. Comparison of the measurements performed in deoxygenated solutions indicated that the phosphorescence lifetimes of the free and the incorporated (NP) forms of all Oxyphors are almost the same (Table 2). In all other tested oxygen environments, the measured lifetimes in the NPs were considerably longer (over an order of magnitude) than for the free form of the Oxyphors, possibly due to the 'pro-

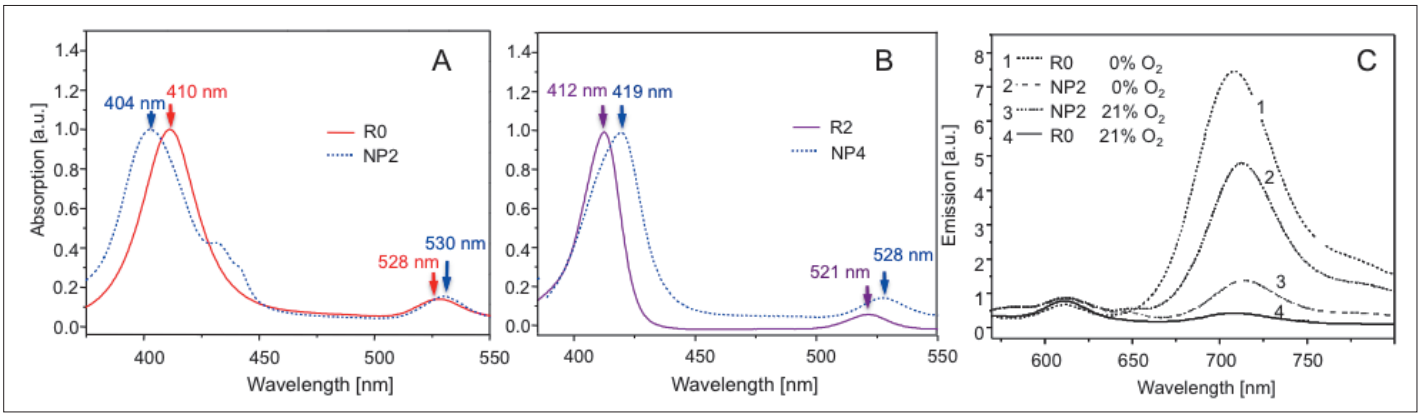

Fig. 3. Absorption and emission spectra of the tested compounds. A), B): Normalized absorption spectra of representative nanoparticle formulations (NP2 and NP4) and free Oxyphors **R0** and **R2** in PBS. C) Emission spectra: NP2 and **R0** (both c = 0.003 g/l) in PBS at 0% or 21% oxygenation conditions.

tective' environment of the polysaccharide nanoparticles.

The calculations of *Rho* (ρ, the ratio of the phosphorescence lifetime of a sensor in a deoxygenated solution to its lifetime in oxygenated solution) and *Alfa* (α, the ratio of ρ for the encapsulated form of the Oxyphor to that of their free form) were performed for various oxygenation conditions (see Table 3 and Fig. 4). The results indicate that the tested NPs are sensitive oxygen sensors since, in the presence of only 5% oxygen, the lifetime is about 4-fold (NP2), 9-fold (NP1 and NP3) or 13-fold (NP4) reduced as compared to the results obtained with deoxygenated solutions. Nevertheless, the sensitivity of Oxyphors to oxygen decreased significantly after the incorporation in NP, *i.e.* approximately 10-fold for NP1, NP3, and NP4, and 5-fold for NP2 (Fig. 4). Nevertheless, the phosphorescence lifetime decreased to around 7–17 µs for the air-saturated nanoparticle formulation, which indicates an efficient quenching of the phosphorescence by molecular oxygen. This change of lifetime is such that the oxygen concentration can be measured in aqueous solutions with a precision ranging between 10 and 20%, for oxygen concentrations ranging between 0% and 25% (error due to the measurement of the lifetime are not taken into consideration).

It is of interest to note that the quenching by molecular oxygen was found to be rapidly and completely reversed by subsequent bubbling of N_2 through the nanoparticle suspension. This observation enables us to exclude processes related to an oxidation of the constituents of the nanoparticles.

The relatively small size of a colloidal nanoparticle is advantageous for its cellular uptake and distribution as compared to other nanoprobes, which are frequently larger. Their small size also provides a large surface-to-volume ratio and a reduced distance over which the oxygen must diffuse to reach the dyes, which leads to the excellent response time we have observed.

It is also interesting to note that, in all cases, the so-called oxygen diffusivity coefficient α was found to remain constant for all NP formulations under all the tested oxygenation conditions. This observation suggests that the reduced oxygen sensitivity induced by the incorporation of Oxyphors in NPs is more likely to be due to the physico-chemical properties of the NPs than to a reduction of oxygen diffusivity. Performing such measurements at different temperatures may provide useful information to address this issue.

The large optical absorption, phosphorescence quantum yield, and acceptable

Table 1. Chitosan-based colloidal particles (nanoparticles) listing the polyelectrolyte complex partner polyanion, the entrapped Oxyphor species, their concentrations and the particles zeta potential in their formulation medium.

Code	Polyanion[a]	Oxyphor	Oxyphor concentration [mg/l]	Zeta potential [mV]
NP1	Heparin	**R0**[b]	60	+/–0
NP2	CMA	**R0**	128	–40
NP3	TPP	**R2**[b]	198	+20
NP4	CS	**R2**	280	+45

[a]Type of polyanion carrier: CMA-carboxymethy amylase; TPP-tripolyphosphate; CS-hondroitin sulfate A; [b]Oxyphor **R0**: Pd-meso-tetra(4-carboxyphenyl)porphyrin]; Oxyphor **R2**: Pd-meso-tetra(4-carboxyphenyl)porphyrin dendrimer.

Table 2. Phosphorescence lifetimes of free Oxyphors **R0** and **R2** and their incorporated forms in NPs in PBS. n.m.: not measured.

Compound	Phosphorescence lifetime [µs] (t_{mean} ± SD*t)				
	0%	5%	10%	15%	25%
NP1	242[a] ± 35	58 ± 9	39 ± 6.7	27.0 ± 5.7	11.2 ± 3.4
NP2	336 ± 60	35 ± 9	21.1 ± 5.1	13.8 ± 2.4	7.4 ± 2.3
R0	363 ± 39	10.5 ± 3.7	4.8 ± 1.2	3.2 ± 0.9	1.9 ± 0.4
NP3	287 ± 55	71 ± 8	37.7 ± 5.6	31.5 ± 9.5	17.0 ± 4.5
NP4	345 ± 32	121 ± 14	62.7 ± 4.9	52.3 ± 5.6	n.m.
R2	282 ± 45	7.7 ± 2.4	5.1 ± 0.9	2.7 ± 0.7	n.m.

[a]Each value is the average of at least 2 independent experiments. The values are given in µs with standard deviations multiplied by student's t-distribution. Measurements were conducted at room temperature in PBS at the atmospheric pressure.

oxygen sensitivity of the tested chitosan-based NPs suggest that this type of formulation is promising to measure the pO_2 in biological systems. For the time being the use of the NP formulations of the oxygen sensors used here did not lead to a strong reduction in phototoxicity. The next steps will consist of further nanoparticle development and assessment of their (photo) toxicity *in vitro* and *in vivo*.

Experimental

Chemicals and Reagents

Oxyphor **R0** [Pd-meso-tetra(4-carboxyphenyl)porphyrin] and Oxyphor **R2** [Pd-meso-tetra(4-carboxyphenyl)porphyrin dendrimer], see Fig. 1A and 1B, were obtained from Oxygen Enterprises Ltd. (Philadelphia, USA). PBS (without Ca^{2+} and Mg^{2+} ions, pH=7.4) was purchased from Gibco (Invitrogen, Scotland). Chitosan middle viscous (Chit), carboxymethyl amylase (CMA), chondroitin sulfate A (CS), heparin and pentasodium triphosphate (aka tripolyphosphate, TPP) were purchased from Sigma-Aldrich (Buchs, Switzerland).

Particle Formation

Chitosan-based colloidal nanoparticles, are polyelectrolyte complexes formed with different polyanions.[28] The Oxyphor derivatives were incorporated into these colloidal particles. All dispersions of colloidal particles were filtered through a 1.2 μm filter, and their ζ-potential was determined by measuring the electrophoretic mobility in a Malvern Nanosizer (Malvern Ltd, Malvern, UK). The batches defined as NP1 and NP2 contained Oxyphor **R0**, whereas NP3 and NP4 contained Oxyphor **R2** (Table 1). This adaptation in the nanoparticle composition was due to the difference in negative charges per molecule of **R0** and **R2**.

Preparation of NP1 and NP2: Under magnetic stirring, a 0.09% solution of heparin was slowly dropped into a 0.05% chitosan solution at pH 4.6, while maintaining the pH between 4.0 and 4.8 by adding 0.1 N HCl. The 'chitosan to heparin' volume ratio in the solution was 2 to 1 in NP1, and 3 to 2 in NP1. A solution of Oxyphor R0 of 1.4% in water at pH 7.0 was added to this colloidal dispersion under continued stirring. During addition, the pH of the dispersion was kept at pH 4.0–4.8 by adding 0.1 N HCl. The addition was stopped at a concentration of 60 mg Oxyphor **R0/l** final dispersion (NP1), and at 128 mg Oxyphor **R0/l** (NP2).

NP3 preparation: Prior to the formation of the colloidal particles, the Oxyphor **R2** was covalently bound to the chitosan by forming an amide bond between the amino group of the chitosan and the Oxyphor **R2** carboxy group. This was performed by employing an aqueous carbodiimide reaction: Oxyphor **R2** was dissolved at 0.38% in 2 ml NaOH. To this solution, 1 ml of 3% sulfo-NHS and 0.4% coupling reagent 1-ethyl-3-(3-dimethyllaminopropyl)carbodiimide hydrochloride (EDC.HCl) was added. After 25 min storage at room temperature, chitosan (3.45 ml, 1.16%) was added. The reaction mixture was stirred at room temperature overnight, then dialyzed (Spectra/Por® Biotech Cellulose Ester Dialysis Membrane MWCO: 25'000 Spectrum Ls Europe B.V., Breda, The Netherlands) against demineralized water. The filtrate was color-free and rejected while the retentate was recovered by freeze-drying. The produced chitosan-Oxyphor **R2** derivative was used to create the colloidal particle dispersion: under magnetic stirring, a 0.1% solution of TPP was slowly dropped into a 0.1% chitosan-Oxyphor **R2** solution at pH 4.6, while maintaining the pH between 4.0 and 4.8 by adding 0.1N HCl. The volume ratio chitosan-Oxyphor **R2** to TPP solution was 6 to 1.

NP4 preparation: Under magnetic stirring, a 0.1% solution of CS was slowly dropped into a 0.025% chitosan solution at pH 4.6, while maintaining the pH between 4.0 and 4.8 by adding 0.1 N HCl. The chitosan to CS volume ratio was 9 to 4 in the solution. Under stirring, a solution of Oxyphor **R2** of 0.01% in water at pH 7.0 was added to this colloidal dispersion. The volume ratio of the colloidal dispersion to Oxyphor **R2** solution was 1 to 1. During addition, the pH of the dispersion was kept at pH 4.0–4.8 by adding 0.1 N HCl. The Oxyphor **R2**-loaded dispersion was concentrated by evaporating the water at 50 °C under normal pressure in a rotary film evaporator. The evaporation was stopped at a concentration of 280 mg Oxyphor **R2/l** in the final dispersion.

Optical Spectroscopy Measurements

UV-VIS and Emission Spectroscopy

Steady-state UV-VIS spectra of the solutions described above were obtained using 1 cm long quartz Suprasil cuvettes (Hellma, Müllheim, Germany) positioned in a two-beam Varian Cary UV-Vis-NIR 500 spectrophotometer (Varian AG, Zug, Switzerland). These optical absorption measurements were performed between 350 and 600 nm with a scan speed of 600 nm/min.

The steady state luminescence emission spectra were recorded with a spectrofluorometer (model LS50B, Perkin-Elmer AG, Massachusetts, USA). The samples, placed in 1 cm long optical path quartz Suprasil cuvettes (Hellma, Müllheim, Germany), were excited at appropriate wavelengths corresponding to their Soret bands (see Fig. 3). The pH of the solutions, was measured with a Schott pH-meter (model CG825) using an InLab™ pH combination electrode (Mettler-Toledo GmbH, Giessen, Germany).

Phosphorescence Lifetime Measurements in Solutions at Different Oxygen Concentrations with the Optical Fiber-based Time-resolved Spectrofluorometer

The oxygen depletion in the studied solutions was obtained by bubbling O_2/N_2 gas mixtures (with known molar concentrations of oxygen, *i.e.* 0%, 5%, 10%, 15% and 25%) during 20 minutes in dedicated 5 cm-long quartz cuvettes (Hellma, Müllheim, Germany) equipped with a gas in/outlet tube. The measurements were performed with the optical fiber-based time-resolved spectrofluorometer described in detail elsewhere (see the block diagram of the setup in Fig. 2A).[27] Briefly, the excitation source was a nitrogen laser-pumped dye laser (LTB Lasertechnik, Berlin, Germany) pulsing at 10 Hz and delivering sub-ns light pulses at 408 nm, operated with the dye 2,5-di-(4-biphenyl)oxazol (BBO, Lambda Physik; Gottingen; Germany). The laser light used to excite the sensors was delivered by a fiber fed into a quartz optical fiber (core diameter 200 μm) by an anti-reflection coated lens and positioned in direct contact with a quartz cuvette outer wall. The same fibre was used to collect the emitted luminescence that was transmitted through a long-pass filter (495 nm) before being coupled into a spectrograph (250IS, Chromex) equipped with a 100 g/mm grating. The centre of the spectral region was set at 700 nm, which gave a spectral recording in the range 630–770 nm. A streak camera (C4334, Hamamatsu Photonics K.K., Japan) was used as a two-dimensional fast detector to record the spectro-temporal images (see Fig. 2B). The sweep speed of the camera was adjusted to capture spectro-temporal images corresponding to the phosphorescence decay times. The data were then processed in order to evaluate the lifetimes of the observed phosphorescence.

The mean lifetime was calculated by fitting a double exponential to the data resulting in a mean of the two lifetimes according to Eqn. (1)

$$\tau_{mean} = \frac{\sum \beta_i \cdot \tau_i^2}{\sum \beta_i \cdot \tau_i} \qquad i = 1, 2 \qquad (1)$$

where the β_i represents the intensities of the individual decay components and the τ_i represents the associated lifetimes.[27]

This approach is justified by the fact that the use of triple, or higher order ex-

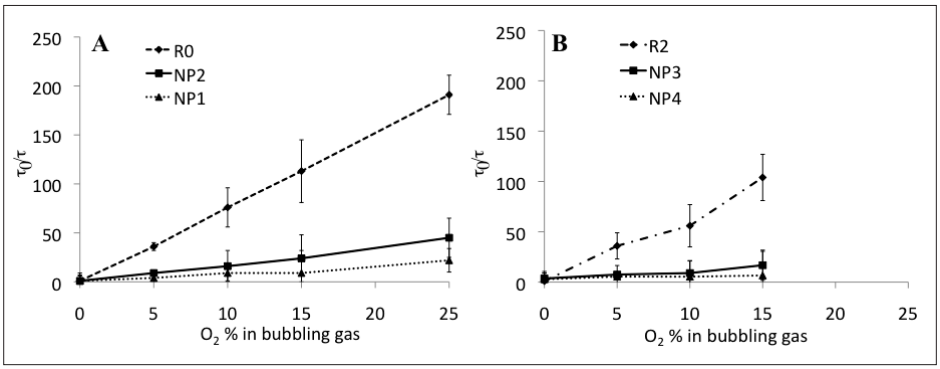

Fig. 4. Stern-Volmer plots of phosphorescence lifetimes of the tested compounds. A) Oxyphor **R0** and **R0**-based nanoparticles (NP1 and NP2), B) Oxyphor **R2** and **R2**-based nanoparticles (NP3 and NP4).

Table 3. Comparison of Rho and Alfa for the free Oxyphors R0 and R2, and their incorporated forms in NPs tested in various oxygenation conditions (room temperature).

Compound	ρ 5%	ρ 10%	ρ 15%	ρ 25%	α 5%	α 10%	α 15%	α 25%
R0	34.6	75.7	113.6	191	1	1	1	1
NP1	4.2	6.1	9.1	21.7	0.12	0.08	0.08	0.11
NP2	9.6	15.9	24.4	45.4	0.28	0.21	0.21	0.24
R2	36.6	56.1	104.4	n.m.	1	1	1	1
NP3	4.0	7.6	9.1	16.9	0.11	0.13	0.08	n.m.
NP4	2.8	5.5	6.6	n.m.	0.08	0.09	0.06	n.m.

ponentials, never improved the residues resulting from a double exponential fitting. In addition, the lifetimes were never mono-exponential, possibly due to the localization of the luminophores in different compartments.

Two more parameters were defined in this study:

1) Rho (ρ), that is the ratio of the phosphorescence lifetime of a sensor in a deoxygenated solution to its lifetime in oxygenated solution.

$$\rho\,[x\%] = \tau\,(0\%\text{ of } O_2) / \tau\,(x\%\text{ of } O_2) \quad (2)$$

Rho defined in this way is a measure of the quenching efficiency.

2) Alfa (α), that is defined as the ratio of ρ for the encapsulated form of the Oxyphor to that of their free form. Thus, α is, at least in part, a measure related to the oxygen diffusivity in the particle, as compared to the solution:

$$\alpha\,[x\%] = \rho_{encapsulated}\,[x\%] / \rho_{free}\,[x\%] \quad (3)$$

Acknowledgments

The authors are grateful for financial support from the J. Jacobi, Trust and the Swiss Foundation (Grant 205320-130518).

Received: June 6, 2011

[1] R. P. Mason, D. Zhao, J. Pacheco-Torres, W. Cui, V. D. Kodibagkar, P. K. Gulaka, G. Hao, P. Thorpe, E. W. Hahn, P. Peschke, *Quart. J. Nucl. Med. Mol. Imaging* **2010**, *54*, 259.
[2] M. R. Horsman, M. Nordsmark, J. Overgaard, *Strahlenther Onkol.* **1998**, *174 Suppl 4*, 2.
[3] P. Nowak-Sliwinska, J. P. Ballini, G. Wagnières, H. van den Bergh, *Microvasc. Res.* **2010**, *79*, 21.
[4] P. Nowak-Sliwinska, J. van Beijnum, M. van Berkel, H. van den Bergh, A. Griffioen, *Angiogenesis* **2010**, *13*, 281.
[5] C. J. Gomer, N. Rucker, A. Ferrario, S. Wong, *Radiat. Res.* **1989**, *120*, 1.
[6] P. Nowak-Sliwinska, G. Wagnières, H. van den Bergh, A. W. Griffioen, *Cell Mol. Life. Sci.* **2010**, *67*, 1559.
[7] O. Mermut, K. R. Diamond, J. F. Cormier, P. Gallant, N. Ho, S. Leclair, J. S. Marois, I. Noiseux, J. F. Morin, M. S. Patterson, M. L. Vernon, *Phys. Med. Biol.* **2009**, *54*, 1.
[8] S. Pervaiz, M. Olivo, *Clin. Exp. Pharmacol. Physiol*. **2006**, *33*, 551.
[9] B. Titz, R. Jeraj, *Phys. Med. Biol*. **2008**, *53*, 4471.
[10] G. Yu, T. Durduran, C. Zhou, T. C. Zhu, J. C. Finlay, T. M. Busch, S. B. Malkowicz, S. M. Hahn, A. G. Yodh, *Photochem. Photobiol.* **2006**, *82*, 1279.
[11] D. W. Hunt, P. Margaron, *Idrugs* **2003**, *6*, 464.
[12] A. Y. Obana, K. Gotho, S. Keneda, T. Nakajima, T. M. Takemura, *Lasers Surg. Med.* **1999**, *24*, 209.
[13] R. D. Shonat, *Adv. Exp. Med. Biol.* **2003**, *510*, 249.
[14] R. P. Dings, M. Loren, H. Heun, E. McNiel, A. W. Griffioen, K. H. Mayo, R. J. Griffin, *Clin. Cancer Res*. **2007**, *13*, 3395.
[15] R. K. Jain, *Science* **2005**, *307*, 58.
[16] P. Gbur, R. Dedic, D. Chorvat, Jr., P. Miskovsky, J. Hala, D. Jancura, *Photochem. Photobiol.* **2009**, *85*, 816.
[17] H. Sterenborg, J. de Wolf, M. Koning, B. Kruijt, A. van den Heuvel, D. Robinson, *Opt. Express* **2004**, *12*, 1873.
[18] S. V. Apreleva, D. F. Wilson, S. A. Vinogradov, *Appl. Optics* **2006**, *45*, 8547.
[19] B. W. McIlroy, A. Curnow, G. Buonaccorsi, M. A. Scott, S. G. Bown, A. J. MacRobert, *J. Photochem. Photobiol. B* **1998**, *43*, 47.
[20] T. K. Stepinac, S. R. Chamot, E. Rungger-Brandle, P. Ferrez, J. L. Munoz, H. van den Bergh, C. E. Riva, C. J. Pournaras, G. A. Wagnières, *Invest. Ophthalmol. Visual Sci.* **2005**, *46*, 956.
[21] P. M. Gewehr, D. T. Delpy, *Med. Biol. Engin. Comp.* **1993**, *31*, 2.
[22] L. W. Lo, S. A. Vinogradov, C. J. Koch, D. F. Wilson, *Adv. Exp. Med. Biol.* **1997**, *428*, 651.
[23] L. W. Lo, C. J. Koch, D. F. Wilson, *Anal. Biochem.* **1996**, *236*, 153.
[24] D. F. Wilson, S. A. Vinogradov, V. Rozhkov, J. Creed, I. Rietveld, A. Pastuszko, *Adv. Exp. Med. Biol.* **2003**, *540*, 1.
[25] D. Moreno, *Sensors Actuators B* **2003**, *90*, 82.
[26] F. Schmitt, L. Lagopoulos, P. Kauper, N. Rossi, N. Busso, J. Barge, G. Wagnières, C. Laue, C. Wandrey, L. Juillerat-Jeanneret, *J. Control Release* **2010**, *144*, 242.
[27] T. Glanzmann, J.-B. Ballini, H. van den Bergh, G. Wagnières, *Rev. Sci. Instrum.* **1999**, *70*, 4067.
[28] P. Calvo, C. Remunan-Lopez, J. L. Vila-Jato, M. J. Alonso, *J. Appl. Poly. Sci.* **1997**, *63*, 125.

Abbreviations

BBO: 2,5-di-(4-biphenyl)oxazol
CMA: carboxymethyl amylase
CS: chondroitin sulfate A
EDC.HCl : 1-Ethyl-3-(3-dimethyllaminopropyl)carbodiimide hydrochloride
NP: nanoparticles
Oxyphor R0: Pd-meso-tetra(4-carboxyphenyl)porphyrin;
Oxyphor R2: Pd-meso-tetra(4-carboxyphenyl)porphyrin dendrimer
PDT: photodynamic therapy
pO_2: oxygen partial pressure
TPP: tripolyphosphate